

EFFECT OF Zn ADDITION IN THE MAGNETIC PROPERTIES OF CO-SUBSTITUTED-Y-TYPE HEXAFERRITE TO BE USED AS RADAR ABSORBING MATERIAL¹

Roberto da Costa Lima²
Magali Silveira Pinho²
Tsuneharu Ogasawara³

Abstract

This work focus mainly on the effect of Zn addition in the magnetic properties of Co₂Y-barium hexaferrite to be used as radar absorbing material. Y-type barium hexaferrites with Ba₂Co₂Fe₁₂O₂₂ and Ba₂CoZnFe₁₂O₂₂ compositions were synthesized by the citrate auto-combustion method, in order to obtain composites with epoxy resin for microwave absorption measurements. The real and imaginary parts of the complex permittivity and permeability were measured. The nanocomposite 80:20 of Ba₂CoZnFe₁₂O₂₂:epoxy resin with 3.0 mm of thickness, showed the best performance as RAM for the X band, with a microwave absorption greater than 90.0 % .

Key words: Y-type hexaferrite; Citrate sol-gel auto-combustion method; TGA; DSC.

EFEITO DE ADIÇÃO DE ZINCO NAS PROPRIEDADES MAGNÉTICAS E ABSORVEDORAS DE RADAR DE HEXAFERRITA TIPO-Y SUBSTITUÍDAS POR COBALTO

Resumo

O objetivo principal deste trabalho é a avaliação do efeito da adição de Zn nas propriedades magnéticas de Co₂-Y-hexaferrita de bário para utilização como material absorvedor de microondas. As composições Ba₂Co₂Fe₁₂O₂₂ e Ba₂CoZnFe₁₂O₂₂ de hexaferritas do tipo Y foram sintetizadas pelo método do citrato por auto-combustão. Compósitos com resina epoxi foram obtidos para as medidas de absorção de microondas, com base na determinação das partes reais e imaginárias da permeabilidade e permissividade complexas. O nanocompósito 80:20 de Ba₂CoZnFe₁₂O₂₂:resina epoxi, com espessura de 3,0 mm apresentou o melhor desempenho como RAM para a banda X, com absorção de microondas superior a 90,0%.

Palavras-chave: Hexaferrita de bário do tipo Y; Método sol-gel de autocombustão; TGA; DSC

¹ Technical contribution to 64th ABM Annual Congress, July, 13th to 17th, 2009, Belo Horizonte, MG, Brazil.

² Doctor of Brazilian Navy Research Institute (IPqM), Rua Ipiru n 2, Praia da Bica, Ilha do Governador, Rio de Janeiro, RJ, Brazil, 21931-090, r.c.lima@uol.com.br, magalipinho@yahoo.com.br

³ Doctor of the Department of Metallurgical and Materials Engineering, Federal University of Rio de Janeiro (COPPE/UFRJ), R J, Brazil, ogasawat@metalmat.ufrj.br

1 INTRODUCTION

Progress in the engineering of electromagnetic wave pollution depends crucially on the development of electromagnetic radiation absorbing materials (RAM).⁽¹⁾ Ferrites have continued to attract much attention over the past 40 years. As magnetic materials, ferrites are not usually replaced because they are relatively inexpensive, chemically stable and show interesting physical and magnetic properties allowing a wide range of technological applications, such as radar absorbing materials.^(1,2) The magnetic and electrical properties of the ferrite are controlled by the preparation conditions, chemical composition, calcination temperature and time and degree of ions' substitution.⁽³⁾

Barium hexaferrites have been classified according to their structures, into five main classes: $\text{BaFe}_{12}\text{O}_{19}$ (M-type), $\text{BaMe}_2\text{Fe}_{16}\text{O}_{27}$ (W-type), $\text{Ba}_2\text{Me}_2\text{Fe}_{28}\text{O}_{46}$ (X-type), $\text{Ba}_2\text{Me}_2\text{Fe}_{12}\text{O}_{22}$ (Y-type) and $\text{Ba}_3\text{Me}_2\text{Fe}_{24}\text{O}_{41}$ (Z-type), where Me represents a divalent ion from the first transition series. All Y compounds ($\text{Ba}_2\text{Me}_2\text{Fe}_{12}\text{O}_{22}$) have planar anisotropy at room temperature, regardless of the metal ion used.

The classical ceramic method for preparing barium hexaferrites requires high calcining temperatures, which induces aggregation of the particles. Afterward, the milling process generally yields non homogeneous mixtures on a microscopic scale and introduces lattice strains in the materials. The use of the sol-gel technique allows to achieve the homogeneity of ions at atomic level in the metallic citrate precursor complex (sol-gel precursor) and lower calcination temperature of barium hexaferrite, besides the action of the nitrate ions as an oxygen source in the gel combustion.⁽⁴⁾

This work focus mainly on the use of TGA analyses for the characterization of the formation of $\text{Ba}_2\text{Co}_2\text{Fe}_{12}\text{O}_{22}$ and $\text{Ba}_2\text{CoZnFe}_{12}\text{O}_{22}$, by the citrate sol-gel combustion process. The sol-gel combustion process is a novel method, with a unique combination of the chemical sol-gel process and the combustion process, based on the gelling and subsequent combustion of an aqueous solution containing salts of the desired metals and some organic fuel, giving a voluminous and fluffy product with a large surface area. This process has the advantages of inexpensive precursors, simple preparation and a resulting nano-sized powder.

In order to obtain the composites for the measurements of the microwave absorption, the powders were mixed with epoxy resin, resulting in the composition 80:20 (wt. %, ferrite:epoxy). The microwave measurements were based on the transmission/reflection method (T/R), using a rectangular waveguide.

2 EXPERIMENTAL

In the citrate sol-gel combustion method, the cations stoichiometric content present in the aqueous solution reacts with the polyfunctional organic acid, citric acid, under controlled pH conditions to give an organometallic precursor complex. The citrate precursor decomposes at temperatures lower than 500°C , allowing barium hexaferrite to be formed at lower temperatures than the required by the powder mixing method, thereby providing an useful way for producing ultrafine homogeneous systems.⁽⁵⁾

Ultrafine $\text{Ba}_2\text{Co}_2\text{Fe}_{12}\text{O}_{22}$ and $\text{Ba}_2\text{CoZnFe}_{12}\text{O}_{22}$ hexaferrite powders were synthesized by this method, using the analytical reagent grade $\text{Fe}(\text{NO}_3)_3 \cdot 9\text{H}_2\text{O}$, $\text{Ba}(\text{NO}_3)_2$, $\text{Co}(\text{NO}_3)_2 \cdot 6\text{H}_2\text{O}$, $\text{Zn}(\text{NO}_3)_2 \cdot 6\text{H}_2\text{O}$ and monohydrate citric acid, in stoichiometric molar ratio. The preparation of the solutions was carried out weighting solids and placing then in a round botton vessel. Bidistilled water was added to each one, under agitation, until total dissolution of solids.

The mixed solution containing the desired cations and citric acid was heated up to 80°C . Ammonia solution was added drop wise into the solution to make it neutral or slightly alkaline (pH=7.5), for subsequent precipitation of the expected organometallic complex, that pops up after the water evaporation. Each of several key-metal cations reacted with citric acid, under

controlled pH conditions, to give the respective metal citrate, making up an homogeneous joint metallic citrate precursor complex.

The mixed solution was rotoevaporated under vacuum at 100°C to produce a highly viscous gel, and then ignited at approximately 250°C, temperature at which self-burning took place in accordance with the pre-determined combustion temperature, giving rise to loose powders.⁽³⁾ The calcination was performed using the following heating schedule: 2°C/min up to 410°C, establishing a plateau for 1 hour, 10°C/min up to the final sintering temperature with a residence time of 4 h at the sintering temperature. The material was then cooled to room temperature at a rate of 10°C/min. The obtained powders were air calcined during 4h at 850, 950 and 1,000°C after heating up at a rate of 10°C/min. Then, the furnace was cooled down at 10°C/min to the room temperature.⁽⁵⁾

The Ba₂Co₂Fe₁₂O₂₂ and Ba₂CoZnFe₁₂O₂₂ crystalline phases formation were investigated by X-ray diffraction (XRD), X-ray fluorescence (XRF), scanning electron microscopy (SEM), vibration sample magnetometry (VSM) and thermogravimetric analysis (TGA).

The calcined products were subjected to X-ray diffraction, with CuK α radiation, in order to assure the formation of the Y-type barium hexaferrite crystalline phase. A PANalytical X'Pert PRO X-ray diffractometer with a step speed of 1°/min, in the θ -2 θ Bragg-Brentano geometry was employed.

X-ray fluorescence (XRF) measurements were carried out by using a Phillips model PW 2400 sequential spectrometer. This quantitative method was used to determine the stoichiometry of the ferrite samples, which were analyzed in the form of a fused bead using lithium tetraborate flux.

The TGA analyses were carried out in a Schimadzu-50 with heating rates of 10°C/min, in static air.

The 4500 VSM of EG & G Princeton Applied Research was used to measure the magnetic hysteresis loops.

The microwave measurements conducted in this work were based on the Transmission/Reflection method (T/R) using a rectangular waveguide as the confining medium for the samples. Using the data obtained (μ' , μ'' , ϵ' and ϵ'' values) from each of the samples measured, an expected prediction of the microwave reflectivity levels for the sheet absorbers was made by illustrating the values of reflectivity (dB) *versus* frequency (GHz), using the HP 8510 network analyzer system. The materials were analyzed for the frequency range 8.2-12.4 GHz (X-band).⁽⁶⁻¹¹⁾

3 RESULTS AND DISCUSSION

Figure 1 illustrates the TGA and DSC curves of the precursor gel of the correspondent Ba₂CoZnFe₁₂O₂₂. The TGA curve exhibits two mainly distinct weight loss steps. The first one in the temperature range of approximately 50-100°C, which is accompanied by a weak endothermic peak between 50-120°C in the DSC curve, corresponds to the loss of the residual water and volatiles. The second weight loss of ~60 % between 100 and 210°C exhibited as an abrupt fall in the TG plot, it is an evidence of the citrate decomposition during the self-combustion process, which is accompanied by the large exothermic peak in the DSC curve, corresponding to the metal oxidation. The combustion temperature was determined as approximately 230°C. From 210 to 400°C, the approximately 5% weight is due to the oxidation reaction of the residual carbon. For temperatures above 400°C, no more weight loss was observed. Based on this result, the gel was calcined at 410°C.

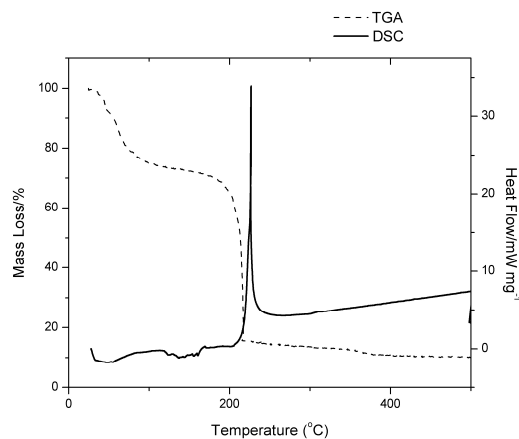


Figure 1. DSC-TGA curves of the dried gel correspondent to $\text{Ba}_2\text{CoZnFe}_{12}\text{O}_{22}$.

Figure 2 illustrates the influence of the calcination temperature on the crystalline phase formation of $\text{Ba}_2\text{CoZnFe}_{12}\text{O}_{22}$.

The use of the lower temperature (850°C) resulted in the presence of second phases, such as $\gamma\text{-Fe}_2\text{O}_3$ (JCPDS 00-089-5894). XRD analyses also indicated that at 950°C , $\text{Ba}_2\text{CoZnFe}_{12}\text{O}_{22}$ became clearly the predominant phase, according to JCPDS 00-044-0207 and for this reason, it was selected as the economically ideal calcination temperature, although second phases' trace amounts undetectable by XRD analysis, may be presented. The average particle size lower than $1\ \mu\text{m}$, was determined by the Scherrer equation. The X-ray diffraction curve of $\text{Ba}_2\text{Co}_2\text{Fe}_{12}\text{O}_{22}$ did not show any difference from the $\text{Ba}_2\text{CoZnFe}_{12}\text{O}_{22}$ one, making its presentation not necessary.

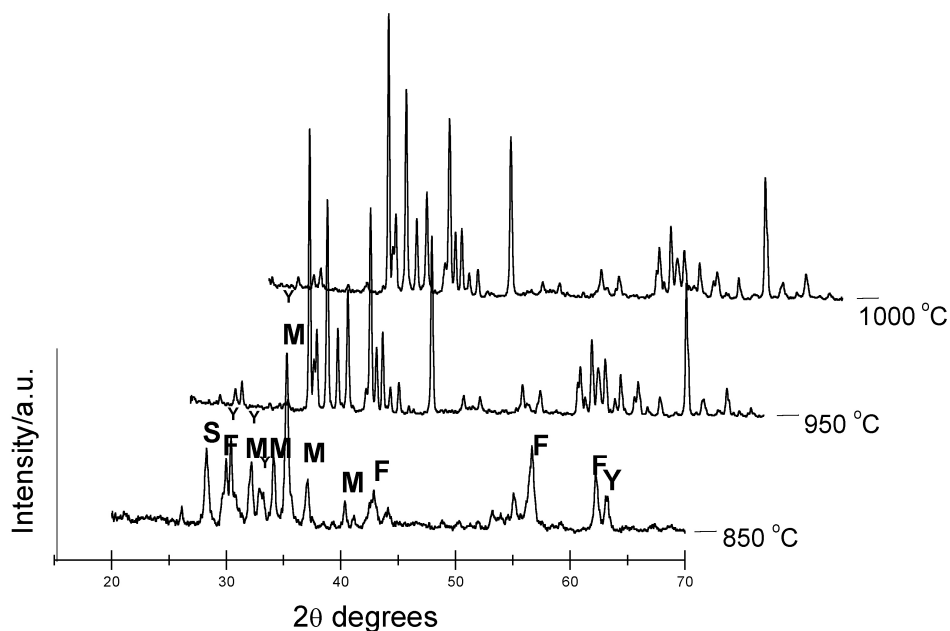


Figure 2. X-Ray diffraction curves for $\text{Ba}_2\text{CoZnFe}_{12}\text{O}_{22}$ powders calcined at different temperatures, with Y and M hexaferrites plus S= BaFe_2O_4 and F= $\gamma\text{-Fe}_2\text{O}_3$.

Results from X-ray fluorescence analysis (XRF) confirmed that the powders synthesized by the self-combustion sol-gel method and calcined at 950°C achieved the

planned stoichiometry. The presence of carbon was not detected even in trace amounts, indicating the total elimination of the organic precursor, favoring the desired formation of $\text{Ba}_2\text{Co}_2\text{Fe}_{12}\text{O}_{22}$ and $\text{Ba}_2\text{CoZnFe}_{12}\text{O}_{22}$ single phases.

The hysteresis curves for Y-type barium hexaferrites fired at 950 °C are illustrated in Figure 3. The magnetization curves show typical feature of magnetically soft ferrites. The saturation magnetization M_s was obtained by extrapolating $M(1/H)$ - curves to $1/H = 0$, resulting in the value of 33 emu/g for $\text{Ba}_2\text{Co}_2\text{Fe}_{12}\text{O}_{22}$ and 22 emu/g for $\text{Ba}_2\text{CoZnFe}_{12}\text{O}_{22}$.

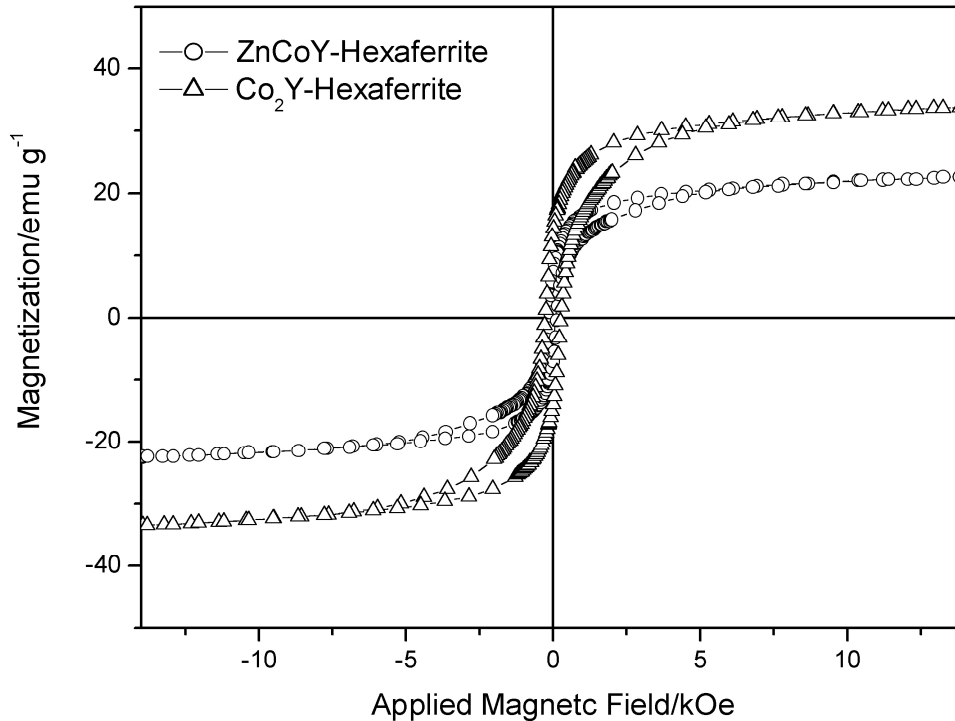


Figure 3. Hysteresis curves of $\text{Ba}_2\text{Co}_2\text{Fe}_{12}\text{O}_{22}$ and $\text{Ba}_2\text{CoZnFe}_{12}\text{O}_{22}$.

According to the literature, the addition of zinc ions improves the complex permeability of the Y-type magnetic ceramics, making possible its use as a RAM for X/Ku bands.⁽¹¹⁾ Moreover, as the particle size is in nanoscale and the discrete energy level spacing is in the energy range of microwave, the electron can absorb the energy as it leaps from one level to another, which may lead to the increment of attenuation.⁽⁷⁻⁹⁾

The effect of Zn addition on the frequency dependence of complex permittivity and permeability for epoxy resin composites with $\text{Co}_2\text{-Y}$ and CoZn-Y barium hexaferrites in the frequency range 8.2-12.4 GHz, is illustrated in Figures 4 and 5.

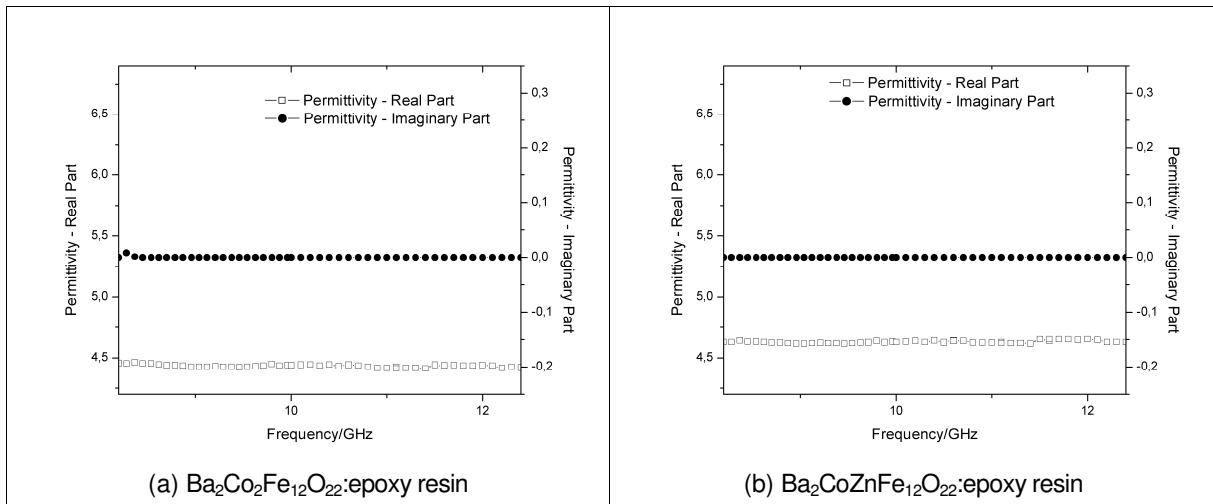


Figure 4. Frequency dependence of complex permittivity for the composites (a) $Ba_2Co_2Fe_{12}O_{22}$:epoxy resin and (b) $Ba_2CoZnFe_{12}O_{22}$:epoxy resin.

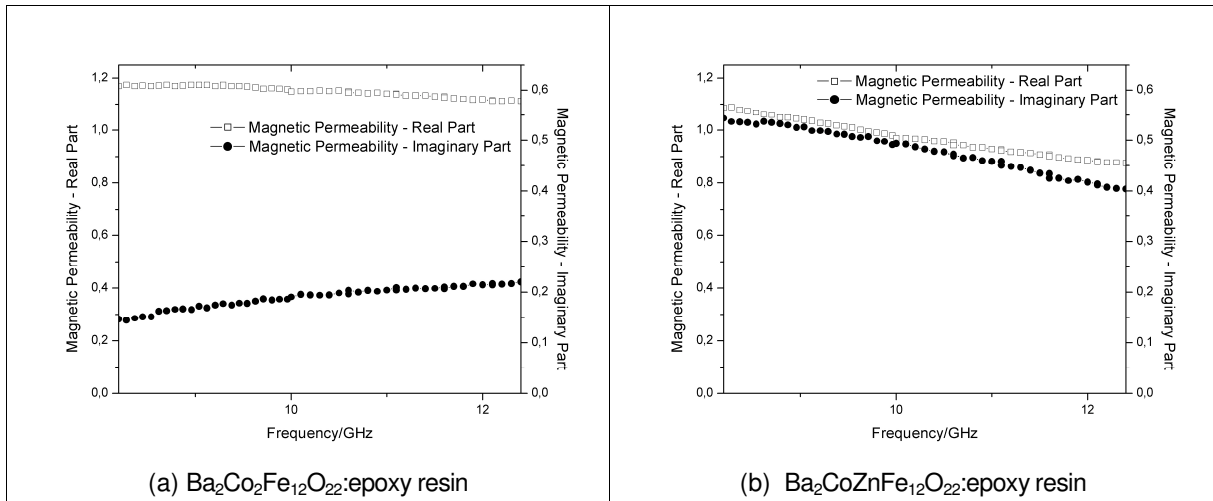


Figure 5. Frequency dependence of complex permeability for the epoxy composites with (a) $Ba_2Co_2Fe_{12}O_{22}$ and (b) $Ba_2CoZnFe_{12}O_{22}$.

It can be observed an increase of the imaginary part of the permeability (μ'') with Zn addition, for the whole range of frequency analyzed.

Figure 6 shows the frequency dependence of dielectric loss (ϵ''/ϵ') and magnetic loss (μ''/μ') at the range of 8.0 – 12.0 GHz (X-band), for the epoxy composites.

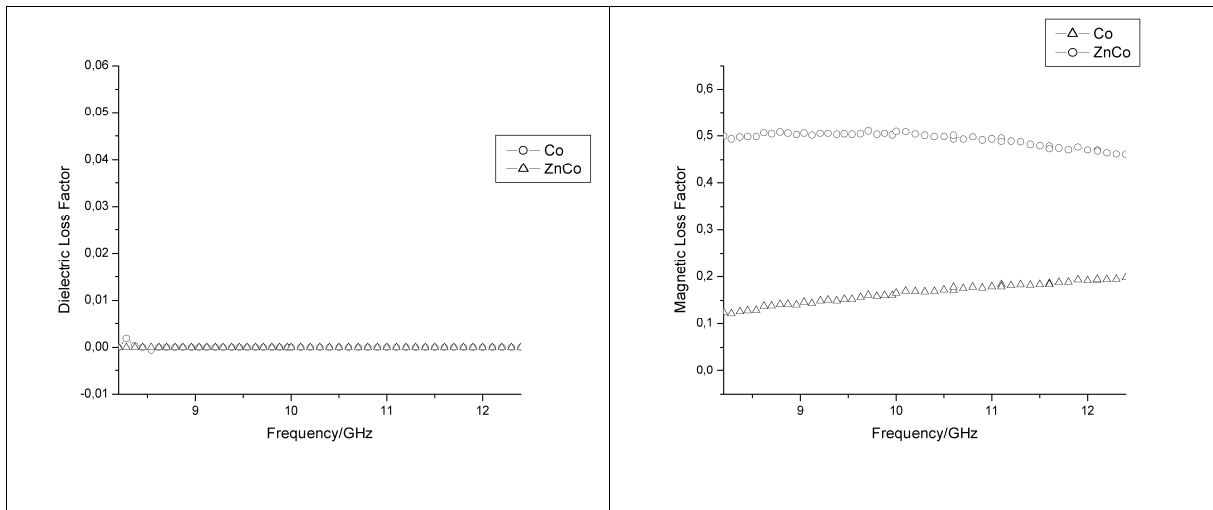


Figure 6. Frequency dependence of dielectric and magnetic losses for the epoxy composites at X-band.

As can be seen from Fig. 6, the dielectric losses are much smaller than the magnetic ones, with values close to zero. For the whole range of frequency analyzed, the magnetic losses are higher than dielectric ones. The change of these losses with frequency may explain the performance of the absorbers, illustrated by the reflectivity curves in Fig. 7, for the composites with thickness of 3.0 mm.

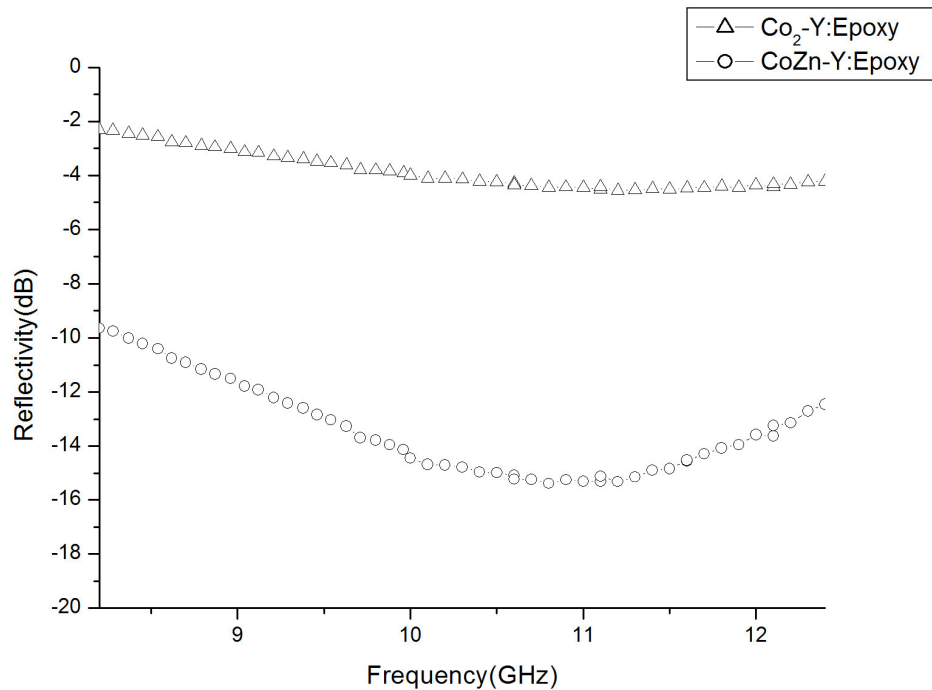


Figure 7. Reflectivity curves for 80:20 (weight %) $Ba_2Co_2Fe_{12}O_{22}$ and $Ba_2CoZnFe_{12}O_{22}$ composites 3.0 mm thick, for X-band.

From Fig. 7, the increase in the permeability loss resulted in an higher microwave attenuation, with a microwave absorption greater than 90.0 % for the frequency range 8.0-12.0GHz, which can be attributed to the addition of Zn.

4 CONCLUSIONS

Nanometric $\text{Ba}_2\text{Co}_2\text{Fe}_{12}\text{O}_{22}$ and $\text{Ba}_2\text{CoZnFe}_{12}\text{O}_{22}$ powders were synthesized by the self-combustion sol-gel method at a lower temperature (950 °C) than the required by the conventional ceramic mixing process (1200 °C).

The total elimination of the organic precursor was assured by XRF analysis, confirming the TGA results.

It was observed that the Zn addition resulted in a reduction of approximately 10 emu/g in the saturation magnetization, which is strongly dependent on the amount of Zn^{2+} that substitute Co^{2+} ions that, in this case, distorted the crystalline field and consequently decreased M_s .

The complex permittivity spectrum showed no significant variation with frequency in the frequency range 8.2-12.4 GHz.

In the complex permeability spectrum, it was observed an increase of the imaginary part of the permeability (μ'') values with Zn addition that, consequently, increased the magnetic loss. The highest magnetic loss of the $\text{Ba}_2\text{CoZnFe}_{12}\text{O}_{22}$ composite 3.0 mm thick, resulted in a microwave absorption greater than 90.0 % (reflectivity values less than -10 dB) for the frequency range 8.2 –12.4 GHz, allowing its application as a good broadband RAM for X-band.

Acknowledgments

The authors gratefully acknowledge Prof. Mirabel Cerqueira Rezende of AMR-IAE for the reflectivity measurements and Prof. Manoel Ribeiro da Silva IF-UFRJ for the VSM analyses, as well as to CNPq, CAPES and FAPERJ for financial support.

REFERENCES

- 1 HUANG, J.; ZHUANG, H.; LI, W. Synthesis and Characterization of Nanocrystalline $\text{BaFe}_{12}\text{O}_{19}$ Powders by Low Temperature Combustion. *Mater. Res. Bull.*, 38, p. 149-159. 2003.
- 2 PINHO, M.S.; GREGORI, M.L.; NUNES, R.C.R.; SOARES, B.G. *Eur. Polym. J.*, 38, p. 2321-2327. 2002.
- 3 HAIJUN, Z.; XI Y.; LIANGYING, Z. J. The Preparation and Microwave Properties of $\text{Ba}_2\text{ZnCo}_2\text{zFe}_{12}\text{O}_{22}$ Hexaferrites. *Eur. Ceram. Soc.*, 22, p. 835-840. 2002.
- 4 MENTUS, S.; JELIC, D. ; GRUDIC, V. J. *Thermal Anal. Cal.*, 90, p. 393-397. 2007.
- 5 MISHRA, S.K.; PATHAK, L.C. ; RAO, V. Synthesis of Submicron Ba-Hexaferrite Powder by a Self-Propagating Chemical Decomposition Process. *Materials Letters*, 32, p. 137-141. 1997.
- 6 OBOL , M.; VITTORIA, C. Measurement of Permeability of Oriented Y-Type Hexaferrites. *J. Magn. Mag. Mat.*, 265, p. 290–295. 2003.
- 7 BADY, I. Ferrites with Planar Anisotropy at Microwave Frequencies. *IEEE Trans. Microwave Theory Tech.*, MTT-9, p.60-70. 1961.
- 8 NAZAROV, A.V.; COX, R.G.; PATTON, C.E. High Power Microwave Properties of Zn-Y Hexagonal Ferrite—Parallel Pumping Size Effects. *J. Appl. Phys.*, 92, p. 3890-3895. 2002.
- 9 RUAN, S.P.; XU, B.K.; SUO, H.; WU, F.Q.; XIANG, S.Q.; ZHAO M.Y. *J. Magn. Mag. Mat.* 212, p.175-180. 2000.
- 10 HAIJUN, Z.; ZHICHAO, L.; CHENGLIANG, M., XI, Y.; LIANGYING, Z.; MINGZHONG, W. *Mater. Sci. Eng. B*96, p. 289-295. 2002.
- 11 CAFFARENA, V.R.; OGASAWARA, T.; CAPITANEO, J.L.; PINHO, M.S. *Mater. Chem. Phys.* 101, p. 81-86. 2007.